Statistical Mechanics of semi-classical colored Objects

M. Hofmann§, M. Bleicher‖, S. Scherer, L. Neise, H. Stöcker, W. Greiner

Institut für Theoretische Physik, J. W. Goethe-Universität,
D-60054 Frankfurt am Main, Germany

Abstract. A microscopic model of deconfined matter based on color interactions between semi-classical quarks is studied. A hadronization mechanism is imposed to examine the properties and the disassembly of a thermalized quark plasma and to investigate the possible existence of a phase transition from quark matter to hadron matter.

The study of relativistic heavy-ion collisions is motivated to a considerable extend by the search for and the unambiguous observation of a phase transition from confined, hadronic matter to a deconfined state of QCD-matter dubbed the quark-gluon plasma [1, 2].

In the forthcoming experiments at RHIC (and later at LHC), the formation of a zone of quark-gluon plasma is generally expected. The primary stage of a collision at RHIC will be dominated by hard pQCD processes leading to the creation of a tremendous number of quarks and gluons which are believed to form a zone of hot and dense and therefore expectedly deconfined partonic matter. This part of a heavy-ion collision has been described microscopically by partonic cascade models as VNI [3]. However, pQCD is, by definition, only applicable in reactions with large momentum transfer Q^2. At SPS these partonic processes are strongly suppressed as compared to hadronic interactions in the early stage. Here, the strong collective motion of the impinging heavy nuclei may drive the system to temperatures and densities beyond the hadronic level into a deconfined phase. However, in both pictures, partonic or hadronic, the major part of particle production takes place in primary collisions within the first few fm/c when the system is strongly compressed and heated.

Most recently, a combination of partonic and hadronic cascades has been established by connecting the VNI model with the UrQMD model which finally copes with the hadronic secondary interactions [4].

§ present address: Sun Microsystems GmbH, Langen, Germany
‖ Fellow of the Josef Buchmann-Foundation

Unfortunately, a possible quark-gluon plasma phase dominated by *soft*, non-perturbative QCD processes which mediates between parton and hadron mode and intrinsically performs the hadronization process is not dynamically treated. The non-perturbative properties of QCD, which are crucial for this transition, impede the applicability of all common approaches to a first-principle description of hadronization. Effective models have to be constructed which allow a numerical calculation of observables by simulating the essential features of non-perturbative QCD. In [5], a dynamical approach based on the Nambu-Jona-Lasinio model has been presented, in which quarks are propagated on classical trajectories while their effective masses are calculated self-consistently according to the NJL equations of motion. Hadron production is driven by qq and qh collisions. Unfortunately, this approach does not provide confinement and therefore is not suitable for the investigation of heavy-ion collisions. On the footing of the Friedberg-Lee Lagrangian, a similar study has been performed in the chromodielectric model [6] completely respecting confinement. Hadronization is performed by mapping quark-gluon states onto irreducible representations of color $SU(3)$. However, this method is numerically extremely expensive. This prohibits the simulation of heavy-ion collisions.

In this paper we present a semi-classical model which mimics the properties of non-abelian QCD by the means of a two-body color potential between quarks. In addition, a dynamical hadronization criterion is defined which allows for the consecutive migration from quark to hadronic degrees of freedom. The long term objective of this investigation is the unification of the different species of microscopic models, partonic in the initial, hadronic in the final stage of the reaction, into one single model, which finally will allow the simulation of a complete heavy-ion collision including a QGP phase transition. In this paper we shall elaborate the major thermodynamic properties of the so-defined system which will justify the crude approximation by its phenomenological implications. In a subsequent publication we will investigate the dynamical evolution of the model and adopt it to more realistic initial conditions which then will allow to describe heavy-ion collisions.

1. The model Hamiltonian

The colored and flavored quarks are treated as semi-classical particles interacting via a Cornell potential with color matrices [7]. This interaction provides an effective description of the non-perturbative, soft gluonic part of QCD. The Hamiltonian reads

$$\mathcal{H} = \sum_{i=1}^{N} \sqrt{p_i^2 + m_i^2} + \frac{1}{2} \sum_{i,j} C_{ij} V(|\mathbf{r}_i - \mathbf{r}_j|)$$

where N is the number of quarks. Four quark flavors (u, d, s, c) with current masses $m_u = m_d = 10$ MeV, $m_s = 150$ MeV and $m_c = 1.5$ MeV are considered.

The confining properties of $V(r)$ are ensured by a linear increase at large distances r. At short distances, the strong coupling constant α_s becomes small, yielding a Coulomb-type behavior as in QED. This color Coulomb potential plus the confining part is the well known Cornell-potential [8]

$$V(r) = -\frac{3}{4}\frac{\alpha_s}{r} + \kappa\, r \ ,$$

which has successfully been applied to meson spectroscopy. For infinite quark masses this inter-quark potential has also been found in lattice calculations over a wide range of quark distances [9]. For small quark masses, retardation and chromomagnetic effects should be included. This is neglected in the present work. However, the linear behavior at large distances seems to be supported by the success of the string model even for zero quark masses [10].

The color matrix elements C_{ij} regulate the sign and relative strength of the interaction between two quarks/antiquarks, respectively, depending on the color combination of the pair. The matrix C_{ij} in the short range color interaction potential between quarks, $V_{\rm color} = -C_{ij}\frac{3}{4}\frac{\alpha}{r}$, can be calculated from the quark-gluon interaction part of the QCD Lagrangian

$$\mathcal{L}_{\rm int} = \frac{g}{2}\,\bar{\Psi}\lambda_a\gamma_\mu\Psi G_a^\mu$$

on the one-gluon exchange level represented by the Feynman diagram

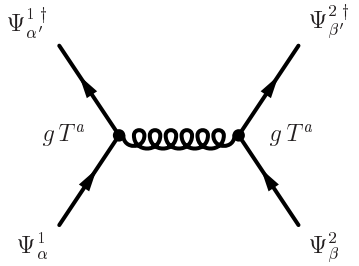

Using the standard fundamental representation of $SU(3)_{\rm color}$ for the quarks and the adjoint representation for the gluons,

$$\vec{q}_R = \begin{pmatrix} 1 \\ 0 \\ 0 \end{pmatrix}, \quad \vec{q}_G = \begin{pmatrix} 0 \\ 1 \\ 0 \end{pmatrix}, \quad \vec{q}_B = \begin{pmatrix} 0 \\ 0 \\ 1 \end{pmatrix},$$

$$T^a = \frac{1}{2}\lambda^a, \quad a = 1, \ldots, 8$$

where λ_a are the Gell-Mann matrices, and separating the quark wave function in the color and Dirac parts,

$$\Psi_\alpha = \psi\,\vec{q}_\alpha$$

the interaction amplitude

$$\mathcal{M}_{\alpha\alpha'\beta\beta'} \sim \frac{g^2}{4}\bar{\Psi}_{\alpha'}\gamma_\mu\lambda^a\Psi_\alpha\,\mathcal{D}^{\mu\nu}_{ab}(q)\,\bar{\Psi}_{\beta'}\gamma_\nu\lambda^b\Psi_\beta$$

separates in color and Dirac parts ($\mathcal{D}^{\mu\nu}_{ab}(q) = D^{\mu\nu}(q)\delta_{ab}$ is the gluon propagator):

$$\mathcal{M}_{\alpha\alpha'\beta\beta'} \sim \bar{\psi}_1\gamma_\mu\psi_1 D^{\mu\nu}(q)\psi_2\gamma_\nu\psi_2\,\vec{q}^{\,\dagger}_{\alpha'}\lambda^a\vec{q}_\alpha\delta_{ab}\vec{q}^{\,\dagger}_{\beta'}\lambda^b\vec{q}_\beta \ .$$

Table 1. Color matrix elements of the 36 different elementary color combinations of the quarks. The matrix elements can be obtained from the scalar products of the corresponding weight vectors

$C_{\rm c}^{\alpha\beta}$	R	G	B	$\overline{B}$	$\overline{G}$	$\overline{R}$
R	-1	$+\frac{1}{2}$	$+\frac{1}{2}$	$-\frac{1}{2}$	$-\frac{1}{2}$	$+1$
G	$+\frac{1}{2}$	-1	$+\frac{1}{2}$	$-\frac{1}{2}$	$+1$	$-\frac{1}{2}$
B	$+\frac{1}{2}$	$+\frac{1}{2}$	-1	$+1$	$-\frac{1}{2}$	$-\frac{1}{2}$
$\overline{\rm B}$	$-\frac{1}{2}$	$-\frac{1}{2}$	$+1$	-1	$+\frac{1}{2}$	$+\frac{1}{2}$
$\overline{\rm G}$	$-\frac{1}{2}$	$+1$	$-\frac{1}{2}$	$+\frac{1}{2}$	-1	$+\frac{1}{2}$
$\overline{\rm R}$	$+1$	$-\frac{1}{2}$	$-\frac{1}{2}$	$+\frac{1}{2}$	$+\frac{1}{2}$	-1

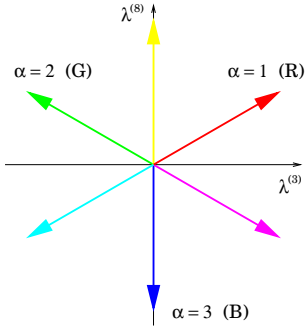

Here, α and β represent the color charges of the incoming quarks, α' and β' of the outgoing quarks. Collecting the color parts in a color factor

$$C^{\rm c}_{\alpha\alpha'\beta\beta'} = \frac{3}{4}\sum_{a=1}^{8} \vec{q}^{\,\dagger}_{\alpha'}\lambda^a\vec{q}_{\alpha}\,\vec{q}^{\,\dagger}_{\beta'}\lambda^a\vec{q}_{\beta} = \frac{3}{4}\sum_{a=1}^{8}(\lambda^a)_{\alpha\alpha'}\,(\lambda^a)_{\beta\beta'}\ ,$$

one can calculate the net amplitude by summing over all possible combinations of in- and outgoing colors. As there is evidence from lattice calculations that there is no color transport over distances larger than $\lambda \approx 0.2\ldots0.3\,$fm, only the commutating diagonal Gell-Mann matrices λ_3 and λ_8 from the Cartan subalgebra of $SU(3)_{\rm color}$ contribute over larger distances. In this Abelian approximation the total color matrix for quark-quark interactions then is given by

$$C^{\rm c}_{\alpha\beta} = \frac{3}{4}\sum_{a=3,8}(\lambda^a)_{\alpha\alpha}(\lambda^a)_{\beta\beta} = \vec{w}^{\,\mathsf{T}}_{\alpha}\vec{w}_{\beta}\ ,$$

where

$$\vec{w}_{\alpha} = \frac{\sqrt{3}}{2}\begin{pmatrix}(\lambda^3)_{\alpha\alpha}\\(\lambda^8)_{\alpha\alpha}\end{pmatrix}, \quad \alpha = 1,2,3\ (R,G,B)$$

are the normalized weight vectors corresponding to the three quark colors in (λ^3,λ^8) space. Imposing a factor -1 at each antiquark vertex in color space yields the color matrix elements for the different color combinations as collected in table 1. They can easily be read off as the scalar products of the weight vectors corresponding to the three colors or anticolors, respectively. Positive values indicate attractive, negative repulsive interactions.

Note that the relative strength of the color matrix elements is rigorously enforced by the requirement of color neutrality of widely separated $q\overline{q}$ and qqq states.

The properties of the interacting quark gas turn out to be independent from the selection of the shape of the potential at small distances, as far as the long distance term is defined properly. Therefore, we shall extend the linear potential to small distances r instead of using the color Coulomb potential at small r, which

brings us in accordance to widely used phenomenological models for hadrons [11, 12].

Regge trajectories yield values of $\kappa_0 \approx 1.1\,\mathrm{GeV/fm}$, while in the string model the string constant is found at $\kappa_0 \approx 0.9\,\mathrm{GeV/fm}$. However, these values were fitted to the properties of isolated strings [13]. In a dense medium, quarks interact with all other color charges. This prohibits the confinement of the field lines into one single flux tube – deconfinement is the consequence. Thus, free string constants κ_0 are not appropriate to calculate the properties of quark matter at high temperatures and densities as expected in heavy-ion collisions [14]. In-medium effects, e. g. interacting color fields, yield an effective increase of the string tension (Casimir scaling) [15]. In the present model κ effectively describes these in-medium effects. It will be treated as a free parameter of the model and should not be identified with the zero temperature value of free strings.

Obviously, a sufficiently high density of color charge carriers will lead to the screening of the the color interaction in the dense medium, and thus color deconfinement results, even in the simple semi-classical toy model presented here. We will discuss this below.

On the other hand, in a less dense and cooler system, all quarks will condense into clusters of two or three (anti-)particles with a total color charge in each cluster of zero. Note that higher quark numbers may also form totally color neutral states which appear to be bound. However, further propagation causes a separation into smaller likewise color neutral subclusters. Therefore, we ultimately obtain bound states which correspond to mesons or baryons.

2. Hadronization

It is now the second request to the model to define a criterion how to map those bound quark states to hadrons. Such a mechanism is essential as the Hamiltonian is not tuned to describe bound and truly confined hadron states. Attempts have been made [16] to do so in a Vlasov approach. Here, we use the straight-forward requirement that the total color interaction from a pair (or a three particle state) of quarks with the remaining system vanishes . Then, these $q\overline{q}$- and qqq-states do no longer contribute to the color interaction of the quark gas (see figure 1). In the present model, this criterion of confinement – which in a numerical simulation of course would never be fulfilled exactly – has been softened by introducing a lower bound for the remaining interaction κ_{min} between the cluster and the residual quark matter beyond which the cluster is declared to be frozen out [17]. It is convenient to measure κ_{min} in units of the natural scale of the model, κ.

$$|\mathbf{F}_{\mathrm{cluster}}| = \left| \frac{1}{N_{\mathrm{cluster}}} \sum_{i \in \mathrm{cluster}} \mathbf{F}_i \right| < \kappa_{\mathrm{min}} = F_{\mathrm{cut}} \cdot \kappa \; .$$

Here,

$$\mathbf{F}_i = \sum_j \mathbf{F}_{ij} = -\sum_j C_{ij} \nabla_j V(|\mathbf{r}_i - \mathbf{r}_j|)$$

gives the total force of the system acting on particle i.

If a bound quark state fulfills the hadronization criterion it will be mapped to an appropriate hadronic state with identical quantum numbers. Spin and isospin of the hadron is randomly chosen according to the probabilities given by the Clebsch-Gordon coefficients.

The mass of the produced hadron is determined by energy and momentum conservation. The total energy of the multi-quark state is given by the expression

$$E_{\mathrm{H}} = \sum_{i \in \mathrm{cluster}} \Big(E_i + \frac{1}{2} \sum_{\substack{j \in \mathrm{cluster} \\ j \neq i}} C_{ij} V(|\mathbf{r}_i - \mathbf{r}_j|) \Big) + \delta E \; .$$

where δE represents the residual energy which was set free due to the field cut-off in the hadronization process and is of the order $\delta E / E \lesssim 10^{-2}$. The momentum of the hadron reads

$$\mathbf{P}_{\mathrm{H}} = \sum_{i \in \mathrm{cluster}} \mathbf{p}_i$$

which yields a hadron mass of

$$M_{\mathrm{H}} = \sqrt{E_{\mathrm{H}}^2 - \mathbf{P}_{\mathrm{H}}^2} \; .$$

Usually the obtained hadron masses will hardly fit to the tabulated pole masses of the known hadrons. Therefore, the quark clusters will preferably be mapped to resonances with a broad mass distribution instead of sharply peaked ground states. In case of multiple possible selections for given quantum numbers we pick one randomly according to mass distributions which are given by Breit-Wigner distributions

$$f(M) \sim \frac{\Gamma^2}{(M - m_0)^2 + (\Gamma/2)^2} \; .$$

Here, m_0 and Γ denote the peak mass and the total decay width of the particle, respectively. To low masses, the distribution is cut-off at a minimal mass to ensure hadronic decay according to the experimentally known branching ratios. In the current version the model discriminates 29 mesonic and 36 baryonic states.

3. Thermodynamic properties of the interacting quarks gas

In the present work, the properties of the interacting quark gas, i. e. of hot quark matter, are studied in complete thermal equilibrium. The system of interacting quarks is *not* an ideal gas, but rather a strongly coupled quark fluid. Therefore, the integration of the partition function cannot be carried out analytically. By adopting the Metropolis algorithm [18], an arbitrary number N_{rep} of N-particle phase space configurations can be generated. The latter configurations are

representations of the equilibrium state of the system. These representations are evaluated by imposing an initial configuration $(\mathbf{x}_i^{(0)}, \mathbf{p}_i^{(0)})$ $(i = 1..N)$ and then repeatedly joggling all coordinates and momenta

$$\begin{aligned} \mathbf{x}_k^{(r)} &\rightarrow \mathbf{x}_k^{(r+1)} = \mathbf{x}_k^{(r)} + \delta\mathbf{x}_k^{(r)} \ , \\ \mathbf{p}_k^{(r)} &\rightarrow \mathbf{p}_k^{(r+1)} = \mathbf{p}_k^{(r)} + \delta\mathbf{p}_k^{(r)} \ . \end{aligned}$$

In each iteration, each displacement $(\delta\mathbf{x}_k^{(r)}, \delta\mathbf{p}_k^{(r)})$ in phase space will cause a change in total energy of the system

$$\Delta E = E^{(r+1)} - E^{(r)} \ .$$

According to the standard Metropolis algorithm, if $\Delta E < 0$, the new configuration is energetically more favorable than the old one and will be accepted. If, on the other hand, ΔE is positive, the new configuration will be accepted with a probability $\exp(-\Delta E/T)$. This allows for a statistical increase of the free energy of the system driven by the "temperature" T. After a sufficient number of iterations the system will enter a stationary state, where further iteration will account for a thermal motion of the sample around the ground state. All configurations can then be identified as representations of the thermalized state.

Now, the ensemble average of any thermodynamical variable O can be approximated by the sum over those representations

$$\langle O \rangle = \frac{1}{N_{\rm rep}} \sum_{k=1}^{N_{\rm rep}} O(\mathbf{x}_i^{(k)}, \mathbf{p}_i^{(k)}) \ , \quad i = 1 \ldots N \ .$$

This enables us to calculate the energy density

$$\epsilon = \frac{1}{V} \langle \mathcal{H} \rangle$$

and – by using the virial theorem – the pressure of the interacting quark gas

$$P = \frac{1}{3V} \left\langle \sum_i \mathbf{p}_i \mathbf{v}_i + \sum_i \mathbf{r}_i \nabla_i V \right\rangle \ .$$

Here $\mathbf{v}_i = \mathbf{p}_i / E_i$ is the velocity of particle i.

In addition to the description of the quark phase we have to cope with the hadronic sector. The produced hadrons are evaporated into the void. The hadron pressure and temperature are assumed to be equal to the quark phase.

We will now assume a system of N quarks in a finite sphere of volume V with all color charges adding up to zero. This system is thermalized at a temperature T according to the previously discussed Metropolis method. A spherical system with a radius of 4 fm contains about 400 quarks and antiquarks at a temperature of 150 MeV. If during the equilibration process quarks form clusters that fulfill the above hadronization criterion they are converted to color neutral hadrons which do no longer interact due to color forces.

3.1. Mixed phase and the equation of state

The first important observable is the number of quarks which are hadronized from a given thermodynamic sample. For high temperatures this quantity should converge to zero, while at $T \to 0$ all quarks should be hadronized due to confinement. The fraction $\xi = N_{\mathrm{h}}/(N_{\mathrm{h}} + N_{\mathrm{q}})$ of hadrons compared to the total particle number in the system therefore should be 1 in this limit. Figure 2 depicts this hadron fraction ξ as a function of the temperature ($\mu = 0$) measured in units of the "critical temperature" T_{C}, where the latter is defined as the temperature of the steepest descent for each set of parameters $(\kappa, F_{\mathrm{cut}})$. A rapid fall-off within $0.2\,T_{\mathrm{C}}$ from a hadron to a quark dominated phase can be observed indicating the existence of a mixed phase during the transition. In case of a true first order phase transition in an infinite volume a sharp discontinuity of this quantity would be expected at T_{C} [19].

A similar continuous transition can be observed in the energy dependence of the quark phase as plotted in figure 3. Here, the energy density ϵ and the pressure p are divided by T^4 and are given for various values of κ and F_{cut} as discussed above. The pressure has been multiplied by a factor of 3. Lattice calculations reveal a similar transition, slightly smoothed for energy density and pressure. [20]. However, our microscopic finite size simulation exhibits an even broader crossover. It is worth to note that the absolute values of lattice calculations for very high temperatures may not be compared to our results as we neglect the contributions of hard gluons.

A functional form of thermodynamic quantities similar to one found here has been parameterized [21, 22] in order to model the *assumed* smooth crossover transition and to study the physical consequences. In accordance to those investigations our microscopic model also reveals a minimum of the equation of state in the phase transition region (see figure 4). However, compared to the case of infinite matter this dip is less pronounced.

The plots in fig. 2 and 3 both reveal a perfect scaling behavior for $F_{\mathrm{cut}} \lesssim 0.01$. This imposes a natural range for the seemingly completely arbitrary parameter F_{cut} which could a priori not be connected to any physical observable.

Despite the conformity in shape, the absolute scale of T_{C} is strongly affected by the particular choice of these parameters. A reduction of F_{cut} to zero will ultimately shift $T_{\mathrm{C}} \to 0$, since hadronization is completely suppressed in this limit. On the other hand, an increase of the string tension, κ, gives rise to an increasing critical temperature T_{C}, revealing a scaling dependence of the form $T_{\mathrm{C}} \sim \sqrt{F_{\mathrm{cut}} \cdot \kappa}$. This can be directly understood from the hadronization mechanism: If any colorless quark cluster ($q\overline{q}$, qqq or, in principle, any multi-quark state) separates from the remaining quarks, we shall always obtain a finite remaining color field between the two quark samples whose strength κ is reduced (screened) compared to the vacuum value. The quark clusters are now assumed to separate sufficiently slowly so that the mediating color field lines can

be considered to confine to an equilibrated flux tube which approximately fulfills the presumptions of a cylindrical MIT bag. In the bag model the field strength κ is connected to the bag constant B according to $\kappa \sim \sqrt{B}$ [13]. On the other hand, the bag pressure for an ideal quark-gluon gas raises as $B \sim T_{\mathrm{C}}^4$. – therefore one immediately obtains $T_C \sim \sqrt{\kappa}$. In our model, the separating cluster is declared a "hadron" if the remaining force drops below the cut-off $F_{\mathrm{cut}} \cdot \kappa$. Applying the flux tube picture as derived form the MIT bag model then yields the previously found dependency for the critical temperature $T_{\mathrm{C}} \sim \sqrt{F_{\mathrm{cut}} \cdot \kappa}$.

While the lattice results predict a critical temperature of $T_{\mathrm{C}} \approx 150\,\mathrm{MeV}$ [20], the natural choices $\kappa = \kappa_0 \approx 1\,\mathrm{GeV/fm}$ and $F_{\mathrm{cut}} = 0.01$ give a much lower value $T_{\mathrm{C}} \approx 90\,\mathrm{MeV}$. As the value for F_{cut} is at the upper bound of the scaling domain, the critical temperature may only be enhanced by increasing the field strength $\kappa > \kappa_0$. The impact of a variation of κ on the thermodynamical properties is visualized in figure 5. In this plot, we further extend the investigations to finite μ and calculate the phase diagram for various κ. First attempts to apply lattice QCD to finite densities [23] seem to support our findings. It is obvious that for high κ the curvature of the lines appears smaller as compared to the curves usually extracted from the MIT bag model. To approach the lattice results of $T_{\mathrm{C}} \approx 140$ MeV for $\mu \to 0$, values $\kappa \gtrsim 2\kappa_0$ are required. For $T \to 0$ the chemical potential than is about 350 MeV so that normal nuclear matter ($\mu \approx 300$ MeV) is safely within the hadronic region. This is in perfect agreement with the above discussion and reflects the finite density character of the quark phase.

The high value found for κ should not come as a surprise: As discussed before, because of in-medium effects an increased string constant (compared to the free value) should be expected.

However, this high value of κ contradicts to the two-particle limit (one quark and one antiquark). The model then turns into the common string model which determines the color field strength to $\kappa = \kappa_0$. In principle, this suggests the introduction of a density and temperature dependence of the string constant. A more qualitative view on the properties of the interacting quark gas shall be provided. However, it should be noted that the hadronization of the QGP is mainly based on quark rearrangements within the blob compared to string fragmentation on the surface of the plasma. This also supports the assumption of particle number conservation in the hadronization process. Hence, we fix the string constant to a medium value of $\kappa = 2\kappa_0$.

The hadronization of the thermalized quark system yields hadron ratios which can be compared at mid-rapidity to those measured in CERN-SPS experiments (see compilation in [24]). Fig. 6 shows the comparison to the outcome in a S+Au collision, assuming a thermal fireball as hadron source. We find a very good agreement in all MM, MB and BB ratios, while the antibaryons seem to be clearly under-predicted. Particle ratios, however, proved not to be a very sensitive observable to test the quality of theoretical models. Fits of a pure hadron gas [24] proved to describe data with a comparable precision as

other thermal or hydrodynamical approaches including a QGP phase transition or several microscopic simulations as UrQMD [25]. However, the analysis of event-by-event fluctuations [26] and of the dynamical properties of the system may yield new insight.

3.2. Dissociation of a quark blob

All results from the last paragraph presume complete equilibration of a finite canonical ensemble which is defined by all possible microscopic representations at a time. One particular representation will always contain fluctuations which may cause the properties of the single representation to deviate strongly from the collective behavior [27]. This effect is emphasized in figure 7 where the average radial force

$$F_{\mathrm{rad}}(r) = \left\langle \sum_i \mathbf{F}_i \, \hat{\mathbf{r}}_i \right\rangle$$

acting on a quark at a distance r from the origin of a spherical thermalized quark blob ($R = 4\,\mathrm{fm}$, $T = 200\,\mathrm{MeV}$, $\mu = 100\,\mathrm{MeV}$) is plotted. In the ensemble average the quarks in the center of the quark matter do not feel any net interaction: color is screened. A net interaction within approximately 1fm from the surface traps the color charges confined within the blob. Moreover, this result is *independent* of the particular shape of the interaction potential as long as it fulfills the symmetry requirements concerning the color charges as given in table 1. Then, within the center of the quark phase all contributions from the potential cancel exactly to zero if the spatial distribution is sufficiently homogeneous. However, this statement holds only for a large number of quark samples. In one single microscopic representation one can find large fluctuations of the net color force on each quark. This is pointed out in figure 8, where the distribution function of the radial color forces $\mathbf{F}_i \, \hat{\mathbf{r}}_i$ acting on quarks *in the center* of the blob is plotted. We obtain an almost perfect Gaussian distribution with a standard deviation $\sigma = 0.5\kappa$ indicating huge fluctuations. Therefore strong inhomogeneities in one single event are to be expected. Hence, the microscopic system will not behave like an ideal quark gas. Due to the color interactions we do not expect that the quark system does expand hydrodynamically, smoothly reducing temperature and density. Instead, these results indicate that during the expansion the quark phase will rupture, and hadrons will condense both from its surface as well as from its interior.

4. Conclusion

We have presented a microscopic description of the deconfinement phase transition by means of a semiclassical interacting quark gas supplemented with a dynamical hadronization criterion. The color interaction potential has been motivated from phenomenological QCD in the abelian approximation. A smooth

crossover was found, comparable to recent lattice results. The phase diagram for finite μ has been calculated. Particle ratios have been compared to experimental results yielding a reasonable agreement. An event-by-event analysis revealed strong fluctuations which initially drive the dissociation process.

Acknowledgments

This work is supported by GSI, BMBF, DFG, Graduiertenkolleg Theoretische und Experimentelle Schwerionenphysik, and the Josef Buchmann Foundation.

References

[1] H. Stöcker and W. Greiner, Phys. Rep. **137**, 277 (1986).
[2] L. McLerran, Rev. Mod. Phys. **58**, 1021 (1986).
[3] K. Geiger and B. Müller, Nucl. Phys. B **369**, 600 (1992).
[4] S.A. Bass, M. Hofmann, M. Bleicher, L. Bravina, E. Zabrodin, H. Stöcker, and W. Greiner, e-print **nucl-th/9902055**, 10pp (1999).
[5] P. Rehberg, L. Bot, and J. Aichelin, e-print **hep-ph/9809565**, 38pp (1998).
[6] C. T. Traxler, U. Mosel, and T. S. Biro, Phys. Rev. C **59**, 1620–1636 (1999).
[7] Nathan Isgur and Jack Paton, Phys. Rev. **D31**, 2910 (1985).
[8] E. Eichten, K. Gottfried, T. Kinoshita, J. Kogut, K.D. Lane, and T.-M. Yan, Phys. Rev. Lett **34**, 369–372 (1975).
[9] K. D. Born, E. Laermann, R. Sommer, T. F. Walsh, and P. M. Zerwas, Phys. Lett. B **329**, 325–331 (1994).
[10] B. Andersson, G. Gustafson, G. Ingelman, and T. Sjöstrand, Phys. Rep. **97**, 31 (1983), no. 2 & 3.
[11] T. Regge, Nuovo Cim. **14**, 951 (1959).
[12] V. N. Gribov, Sov. Phys. JETP **26**, 414–422 (1968).
[13] K. Sailer, T. Schönfeld, Z. Schram, A. Schäfer, and W. Greiner, J. Phys. G **17**, 1005–1057 (1991).
[14] T. S. Biro, H. B. Nielsen, and J. Knoll, Nucl. Phys. B **245**, 449 (1984).
[15] M. Faber, J. Greensite, and S. Olejnik, Phys.Rev. **D57**, 2603–2609 (1998).
[16] A. Bonasera, e-print **nucl-th/9905025**, 11pp (1999).
[17] Matt Crawford and David N. Schramm, Nature **298**, 538–540 (1982).
[18] N. Metropolis, A.W. Rosenbluth, M.N. Rosenbluth, A.H. Teller, and E. Teller, J.Chem.Phys **21**, 1087–1092 (1953).
[19] C. Spieles, H. Stöcker, and C. Greiner, Eur. Phys. J. C **2**, 351 (1998).
[20] F. Karsch, Nucl.Phys. **A590**, 367 (1995).
[21] D. H. Rischke and M. Gyulassy, Nucl. Phys. A **597**, 701–726 (1996).
[22] M. Asakawa and T. Hatsuda, Phys. Rev. D **55**, 4488–4491 (1997).
[23] J. Engels, O. Kaczmarek, F. Karsch, and E. Laermann, e-print **hep-lat/9903030**, 25pp (1999).
[24] P. Braun-Munzinger, J. Stachel, J. P. Wessels, and N. Xu, Phys. Lett. B **365**, 1 (1996).
[25] S.A. Bass, M. Belkacem, M. Brandstetter, M. Bleicher, L. Gerland, J. Konopka, L. Neise, C. Spieles, S. Soff, H. Weber, H. Stocker, and W. Greiner, Phys. Rev. Lett. **81**, 4092 (1998).
[26] M. Bleicher, M. Belkacem, C. Ernst, H. Weber, L. Gerland, C. Spieles, S.A. Bass, H. Stocker, and W. Greiner, Phys. Lett. **B435**, 9 (1998).
[27] M. Bleicher, L. Gerland, S. Bass, M. Brandstetter, C. Ernst, S. Soff, H. Weber, H. Stöcker, and W. Greiner, Nucl. Phys. A **638**, 391–394 (1998).

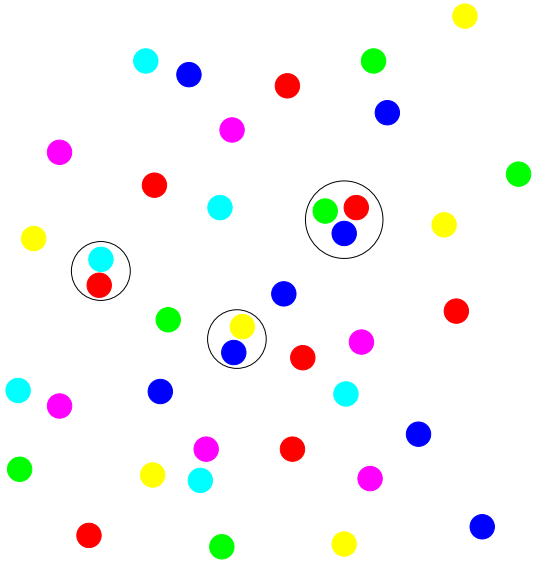

Figure 1. Hadronization of white quark clusters

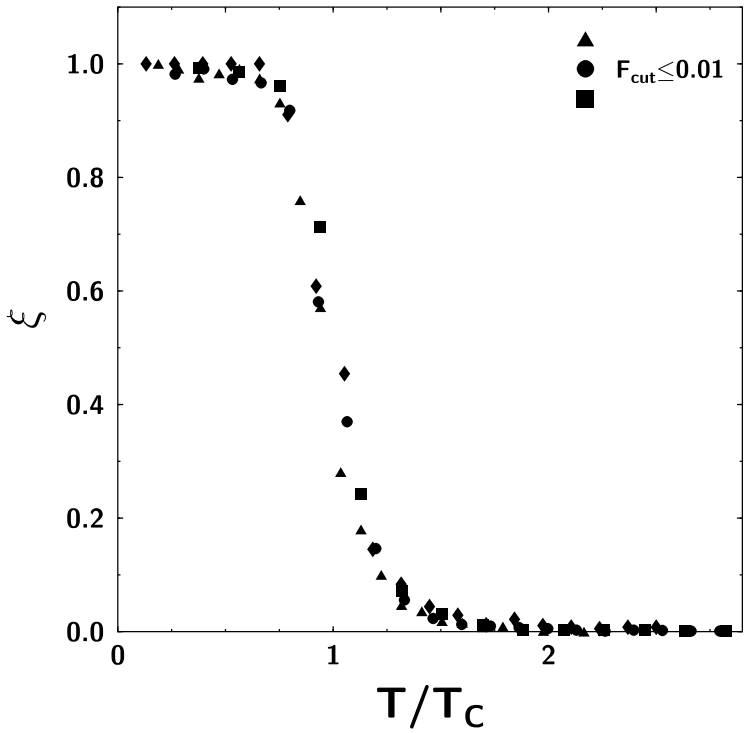

Figure 2. Hadron fraction as a function of temperature in a finite quark blob for various sets of parameters κ and $F_{\rm cut}$. The temperature is measured in $T_{\rm C}$ which is defined for any set of parameters as the temperature of steepest descent with T. The distributions show perfect scaling behavior for $F_{\rm cut} < 0.01$ (black symbols).

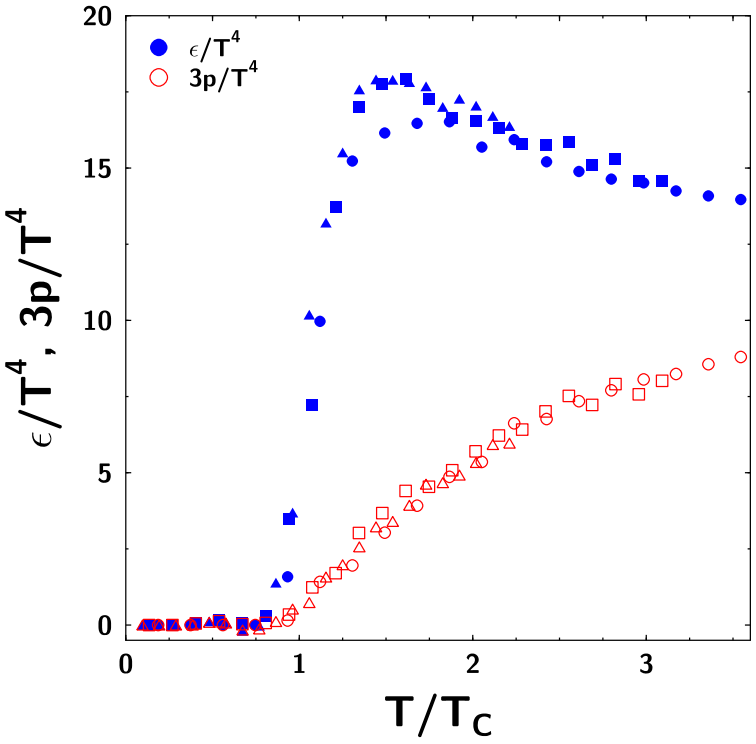

Figure 3. Energy density and pressure of the quark phase as a function of temperature for various sets of parameters κ and $F_{\rm cut}$.

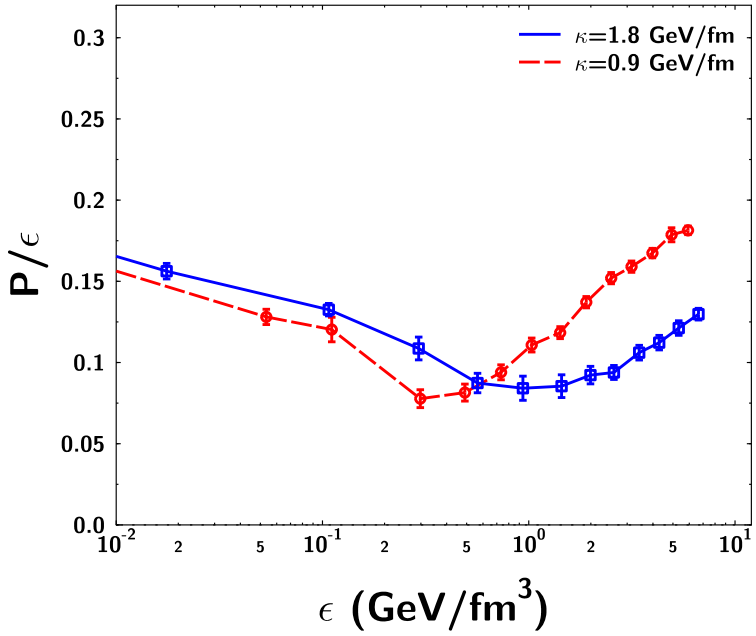

Figure 4. Equation of state for $\kappa = \kappa_0$ (dashed line) and $\kappa = 2\kappa_0$ (solid line). A softening of the EOS around $\epsilon = 1\text{GeV/fm}^3$ is revealed.

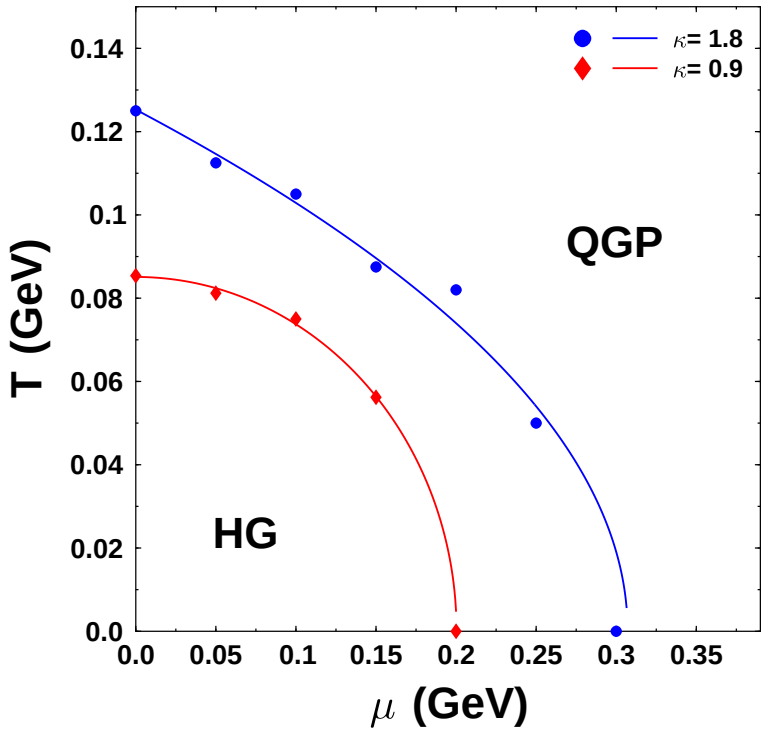

Figure 5. Phase diagram in the T-μ plane for $\kappa/\kappa_0 = 1, 2$. The lines are fits to the calculation.

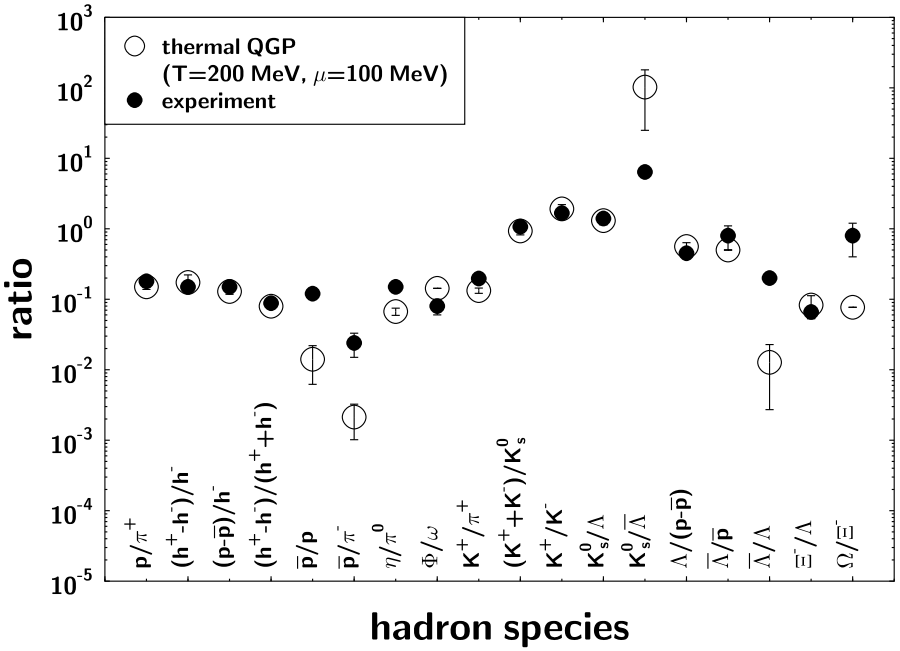

Figure 6. Final state hadron ratios from thermal qMD calculations (open circles) compared to S+Au data at 200 AGeV (full circles, taken from [24])

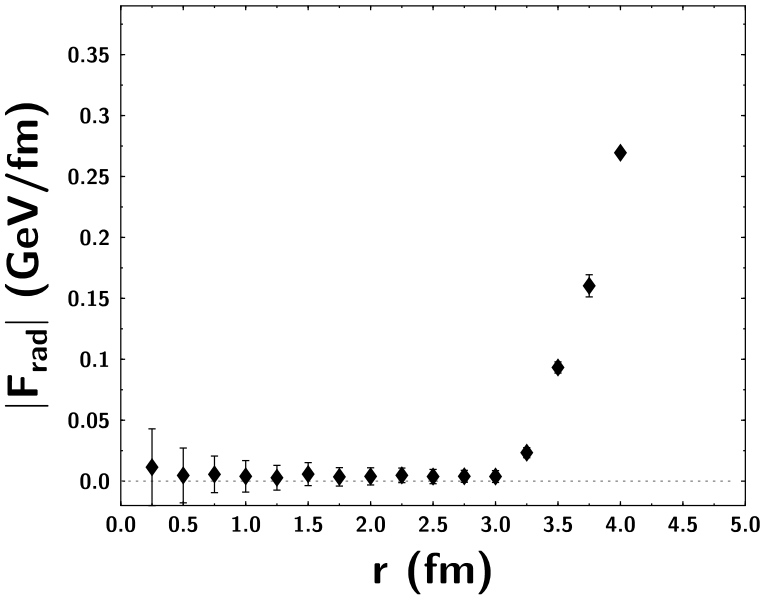

Figure 7. Averaged radial force $|\sum \mathbf{F}\hat{\mathbf{r}}|$ acting on a quark at a distance r within a quark blob of radius $R = 4$fm. In the center the quarks are approximately free. Near the surface they are strongly pulled back into the sphere.

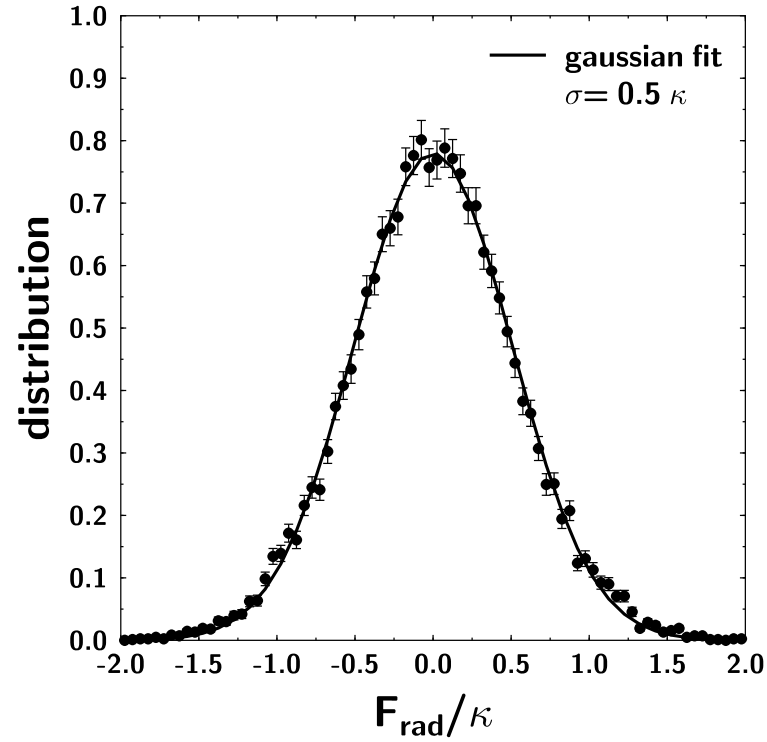

Figure 8. Fluctuations of net radial forces $F_{\mathrm{rad}} = \sum \mathbf{F}\hat{\mathbf{r}}$ acting on a central quark ($r < 1$fm).